journal

J. Am. Ceram. Soc., 89 [3] 1037–1041 (2006)
DOI: 10.1111/j.1551-2916.2005.00789.x

Spectroscopic and Thermal Properties of Ga_2S_3–Na_2S–CsCl Glasses

Luiz C. Barbosa† and Carlos L. Cesar

Department of Quantum Electronics, Institute of Physics Gleb Wataghin, State University of Campinas (UNICAMP), Campinas, SP, Brazil

Italo O. Mazali and Oswaldo L. Alves

Solid State Chemistry Laboratory, Institute of Chemistry, State University of Campinas (UNICAMP), Campinas, SP, Brazil

The synthesis and properties of the vitreous system $(0.75-x)Ga_2S_3$–$0.25Na_2S$–xCsCl, with x varying from 0.1 to 0.2, are presented. Thermal, optical, and structural properties such as density, viscosity, thermal expansion coefficient, glass transition temperature, softening point temperature, refractive index, and absorption coefficient were measured using several techniques: X-ray diffraction, Raman scattering, differential thermal analysis, thermal mechanical analysis, and absorption spectroscopy. This glass system presents a high third-order non-linear optical susceptibility that can be significantly increased by increasing the CsCl content without affecting the low phonon frequency.

I. Introduction

Chalcogenide and chalcohalide glasses have a number of interesting and specific features useful for practical applications, for instance, optical fiber amplifier devices in the 1.3 μm region. Their low phonon frequency (430 cm^{-1}) and high refractive indices (ranging from 2.1 to 2.5 at 589.9 nm) are a prerequisite for long excited state lifetimes, enhancing the pump efficiency.[1–3] In chalcogenides such as the Ga_2S_3–La_2S_3 glass system, however, the temperature of the suitable viscosity coincides with the onset of crystallization, to make drawing of fibers difficult.[4] This drawback can be circumvented by the addition of CsCl to the glass composition. This increases the thermal stability region, allowing fiber to be drawn.[5] On the other hand, Ga_2S_3–Na_2S (GNS) glasses were found to be thermally stable and able to incorporate large amounts of rare-earth ions.[6] A Pr^{3+} GNS chalcogenide glass fiber with a transmission loss of 12 dB/m at 1.31 μm has been fabricated, and a large gain coefficient of 0.81 dB/mW has been achieved.[7]

Chalcohalide glasses of the family Ga_2S_3–Na_2S–CsCl (GNSC) have attracted interest because of the possibility of their use as a host for praseodymium or dysprosium in an optical amplifier for the 1.3 μm wavelength communication window. In this work, the density, phonon frequencies, viscosity, hardness, thermal expansion coefficient, glass transition temperature, absorption, and refractive index of this glass network were measured as a function of the CsCl content. The results show that the refractive index increases with the CsCl content, while the phonon frequencies are maintained at low values, below 440 cm^{-1}. The third-order non-linear optical susceptibility $\chi^{(3)}$ at 1.3 and 1.5 μm increases significantly with CsCl addition, which is desirable for optical devices.[8,9] Furthermore, the results show that there is no crystallization at temperatures of suitable viscosity for drawing of fibers and that the activation energy for viscous flow at low and high temperatures is approximately the same.

II. Experimental Procedure

(1) Preparation of Sample for Measurement

The $(0.75-x)Ga_2S_3$–$0.25Na_2S$–xCsCl (GNSC) glass system samples, with x varying from 0.1 to 0.2, were fabricated in a silica crucible using a technique described by Marmolejo *et al.*[10] The experimental setup consists of two furnaces horizontally aligned with a silica tube liner passing through both of them. The atmosphere in the silica tube can be controlled under flowing argon conditions. To prevent any loss of sulfur during the melting process, a crucible containing, typically, 20 g of pure sulfur was placed within the silica tube in the first furnace, away from the melting zone (second furnace). The concentration of sulfur vapor across the melting zone was established by the first furnace temperature and the carrier argon gas flow. Melting was achieved at 1173 K for 6 h. After this time, the glass was annealed for 48 h at 673 K. Table I shows the composition of the glass batch (CERAC, 99.99% pure).

(2) Measurement

The compositions of the glasses obtained were analyzed by X-ray fluorescence spectroscopy (EDX-700, Shimadzu, Japan). Raman spectra were measured using the 514.5 nm argon ion laser line with backscattering geometry and a triple Jobin–Yvon spectrometer with multichannel detection (Jobin-Yvon Inc., Edison, NJ). The density was measured by the Archimedes method using deionized water as the bouyancy liquid at 298 K. The thermal properties were measured by differential thermal analysis (DTA, Shimadzu), which provided the characteristic temperatures, and by thermal mechanical analysis (TMA, Shimadzu), which yielded the thermal expansion coefficient and softening temperature, both determined at a 10 K/min heating rate. The viscosity was measured by the parallel plate method of Wilson[11] in a TMA (Shimadzu). The refractive indices were measured over a wide wavelength range, from 580 to 1750 nm, using a manual Rudolph null ellipsometer (model 436, Rudolph

Table I. Nominal Composition of Ga_2S_3–Na_2S–CsCl Glasses

	Composition (mol%)		
Glass	Na_2S	Ga_2S_3	CsCl
GNSC10	25	65	10
GNSC15	25	60	15
GNSC18	25	57	18
GNSC20	25	55	20

GNSC, Ga_2S_3–Na_2S–CsCl.

D. Johnson—contributing editor

Manuscript No. 20590. Received May 23, 2005; approved September 23, 2005.
†Author to whom correspondence should be addressed. e-mail: barbosa@ifi.unicamp.br

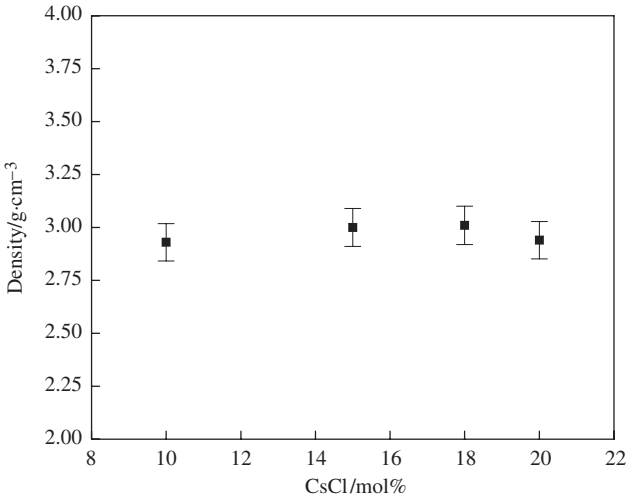

Fig. 1. Ga_2S_3–Na_2S–CsCl glass system density dependence on the CsCl content.

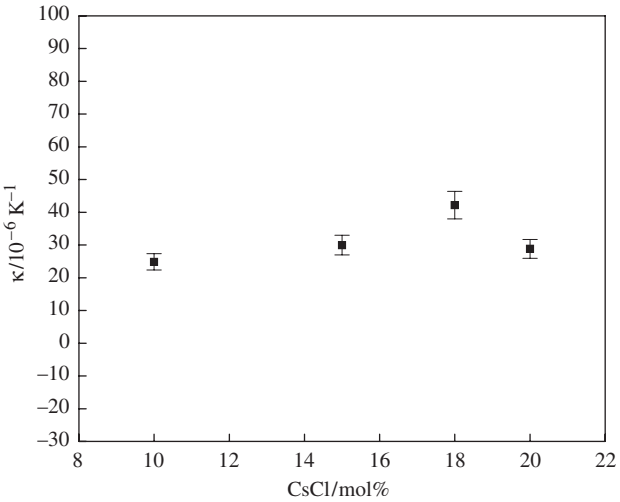

Fig. 3. Thermal expansion coefficient (κ) for the Ga_2S_3–Na_2S–CsCl glass system as a function of the CsCl content.

Instruments, Denville, NJ) with a 150 W tungsten lamp as a light source, with an accuracy of ±0.0005. Interference filters selected the desired wavelength. UV-visible absorption spectra were recorded in the wavelength region from 300 to 2500 nm, using a Perkin–Elmer Lambda 9 spectrophotometer (Wellesley, MA).

III. Results

(1) Glass Formation and Density

The preparation procedure produced bubble-free transparent glasses with high homogeneity and a yellowish color. Owing to the vaporization of CsCl at the melting temperature, the compositions of the glasses obtained were analyzed by X-ray fluorescence spectroscopy. Although it is a semi-quantitative technique, all GNSC glasses showed a reproducible mass loss between 4% and 6%, independent of the CsCl content, indicating that the composition change because of vaporization of CsCl was limited. Similar results were also reported by Ramos *et al.*[12] Figure 1 shows the behavior of the density as a function of the CsCl content.

(2) Thermal Properties

Figure 2 shows the glass transition (T_g) and softening (T_d) temperatures, and Fig. 3 shows the thermal expansion coefficient (κ), all as a function of the CsCl content. Figure 4 presents the thermograms for a series of samples. From **a** to **e,** the CsCl concentration corresponds to 0, 10, 15, 18, and 20 mol%, respectively. Table II displays the thermal properties obtained for this glass system, where T_x is the onset of crystallization temperature.

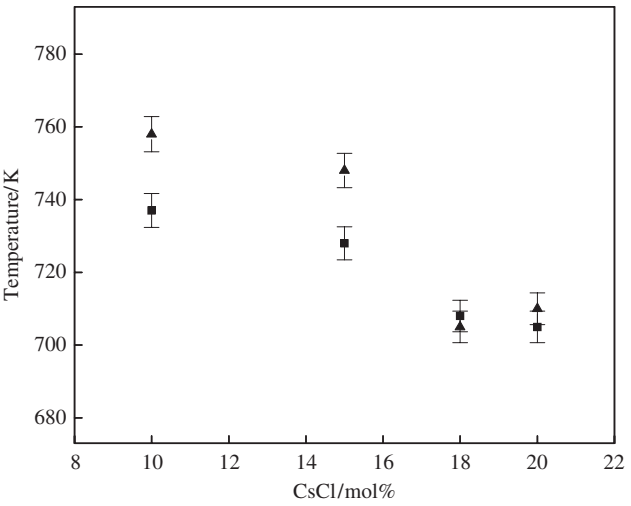

Fig. 2. (■) T_g and (▲) T_d temperatures for the Ga_2S_3–Na_2S–CsCl glass system as a function of CsCl content.

(3) Optical Properties

(A) Absorption: For each composition, the absorption coefficient α was measured using two samples with different thicknesses.[13] The optical gap values were obtained by extrapolation of the square root of the product of the absorption coefficient times the photon energy versus photon energy $[(\alpha E)^{1/2}$ vs $E]$ to the zero absorption coefficient, as also carried out by Tauc *et al.*[14] Figure 5 shows these extrapolations with the corresponding values of the optical gap (Tauc gap, E_T) where $(\alpha E_T)^{1/2} = 0$. There is a clear blue shift of the Tauc gap as the CsCl content increases.

(B) Linear Refractive Index: The results for the linear refractive index n of samples **a** to **d** are presented in Fig. 6. For all samples, the refractive index decreases with increasing wavelength in the 580–1750 nm range. Curve fits of the experimental data were performed using the model proposed by Wemple and DiDomenico.[15] In this model, the refractive index n as a

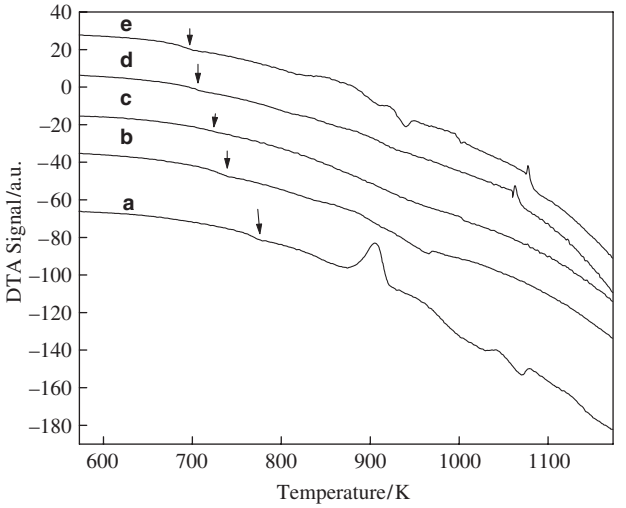

Fig. 4. Thermograms from differential thermal analysis analysis for the Ga_2S_3–Na_2S–CsCl glass system: (a) 0 mol%, (b) 10 mol%, (c) 15 mol%, (d) 18 mol%, and (e) 20 mol % CsCl. The arrows show the glass transition temperature.

Table II. Thermal Properties of a GNSC Glass System

CsCl (mol%)	T_g (K)	T_d (K)	T_x (K)	Density (g/cm^3)	κ (10^{-6} K^{-1})
0	—	—	882	—	31.04
10	737	758	—	2.93	24.85
15	728	748	—	3.00	29.98
18	708	705	—	3.01	42.20

GNSC, Ga_2S_3–Na_2S–CsCl.

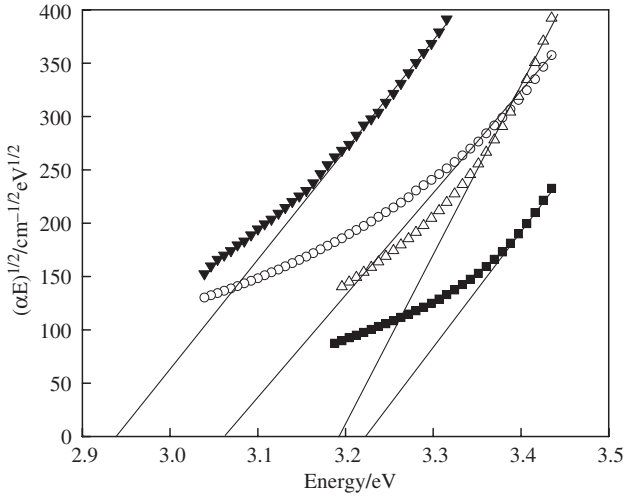

Fig. 5. $(\alpha E)^{1/2}$ versus E plot for samples: (▼) 0 mol% CsCl, (○) 10 mol% CsCl, (Δ) 15 mol% CsCl, and (■) 18 mol% CsCl.

function of the photon energy E is given by

$$\frac{1}{n^2-1}=\frac{E_0}{E_d}-\frac{E^2}{E_0E_d} \tag{1}$$

where E_0 is the average energy gap and E_d is the dispersion energy parameter, related to interband oscillator strength. The resulting values for the two fitting parameters E_0 and E_d are listed in Table III. The E_0 values will be used to estimate the non-linear refractive index in the next section.

(C) Non-linear Refractive Index: The influence of several parameters on the non-linear refractive index of transparent pre-transition and transition metal complexes has been studied

Table III. Data Used to Calculate $\chi^{(3)}$ from the Lines Theory

	n (μm)					$\chi^{(3)}$ (10−12 esu)	
CsCl (mol%)	1.3	1.5	d (Å)	E_0 (eV)	E_d (eV)	1.3 μm	1.5 μm
0	1.386	1.356	2.3	2.56	17.3	0.7	0.5
10	1.431	1.396	2.3	2.11	16.7	1.8	1.1
15	1.484	1.447	2.3	2.14	18.2	2.2	1.3
20	1.435	1.393	2.3	1.68	21.9	5.2	2.2

by Lines.[8,9] In this model, the frequency-dependent non-linear refractive index n_2 is written as

$$n_2(\text{av.})/10^{-13}\text{esu}=25\frac{(f\times f_L)^3d^2(n^2-1)E_s^6}{n(E_s^2-\hbar^2\omega^2)^4} \tag{2}$$

where d is the bond length for the ternary glass (in Å), f is the local-field enhancement factor, $f_L=(n^2+2)/3$ is the Lorentz local-field factor,[9] n is the long-wavelength limit value of the refractive index, and E_s is the effective Sellmeier energy gap. The third-order non-linear optical susceptibility $\chi^{(3)}$ is related to n_2 by the equation[8]

$$\chi^{(3)}(-\omega,\omega,\omega,\omega)=\frac{n}{3\pi}n_2(\text{av.}) \tag{3}$$

From Eqs. (2) and (3), assuming $f=1$ and $E_s=E_o$,[8,9] we have estimated the $\chi^{(3)}$ values at 1.3 and 1.5 μm for the series of samples studied. The refractive index values n used in the calculation correspond to those presented in Fig. 7, and the bond length d was estimated to be 2.3 Å.[16,17] Figure 7 shows the results as a function of the CsCl content. Table III displays the $\chi^{(3)}$ values obtained, together with all the parameters used in its calculation. One can see that $\chi^{(3)}$ is very sensitive to the CsCl content, showing a remarkable increase with increasing concentration.

(D) Raman Spectra: The Raman spectra of the GNSC glasses are presented in Fig. 8. We note two types of vibration modes: the external vibration modes at frequencies below 200 cm^{-1} and internal vibration modes at higher frequencies (200–500 cm^{-1}). One can distinguish two bands related to the external modes: a band at 99 cm^{-1} (band I), which can be attributed to the translation mode (T) of the GaS_4 tetrahedra, and a band at 177 cm^{-1} (band II), which can be attributed to the deformation mode (A_1) of the GaS_4 tetrahedra. At higher frequencies, five bands related to internal modes of the GaS_4 tetrahedra[18] are distinguished: a shoulder situated at 241 cm^{-1} (band III), a band

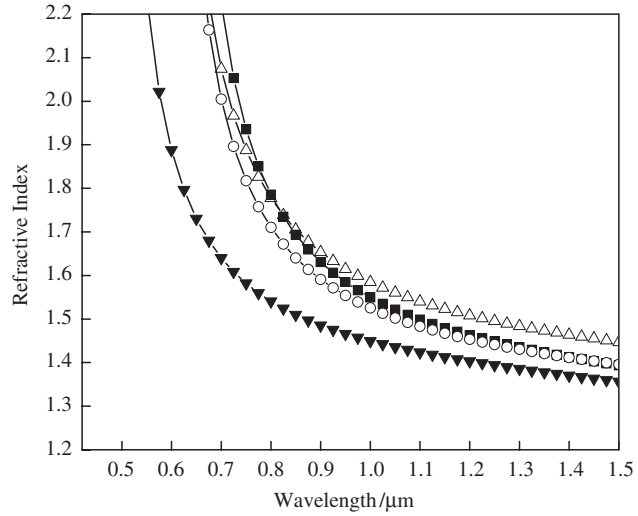

Fig. 6. Linear refractive index as a function of wavelength for (▼) 0 mol%, (○) 10 mol%, (Δ) 15 mol%, and (■) 18 mol% CsCl.

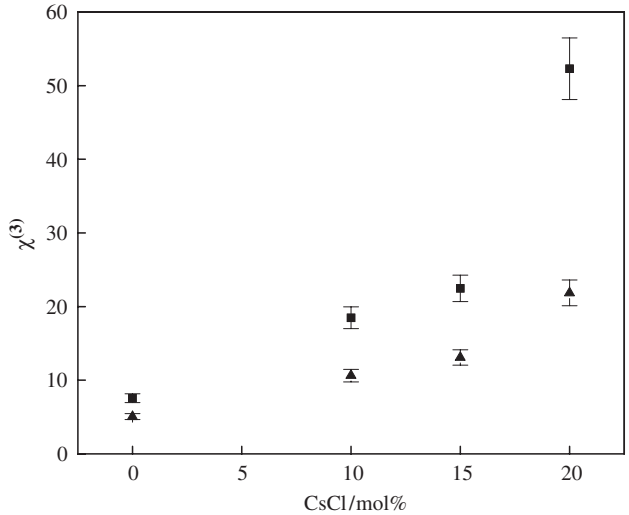

Fig. 7. Third-order susceptibility $\chi^{(3)}$ as a function of the CsCl content for the GNSC glass system at 1.3 μm (■) and 1.5 μm (▲).

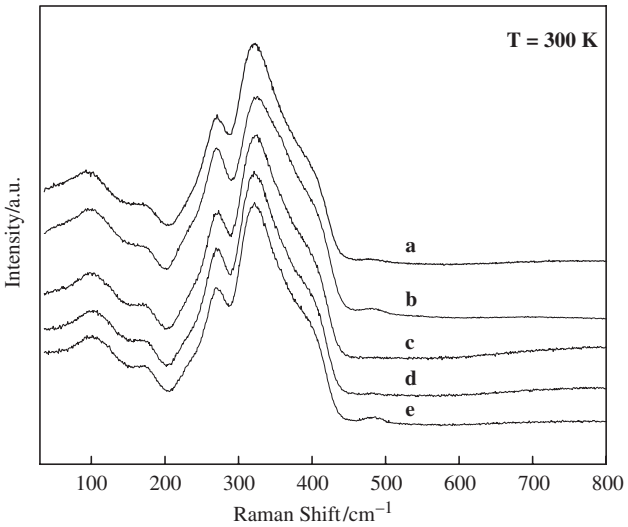

Fig. 8. Raman spectra of the GNSC glass system. The spectra have been arbitrarily shifted vertically for clarity: (a) 0 mol%, (b) 10 mol%, (c) 15 mol%, (d) 18 mol%, and (e) 20 mol% CsCl.

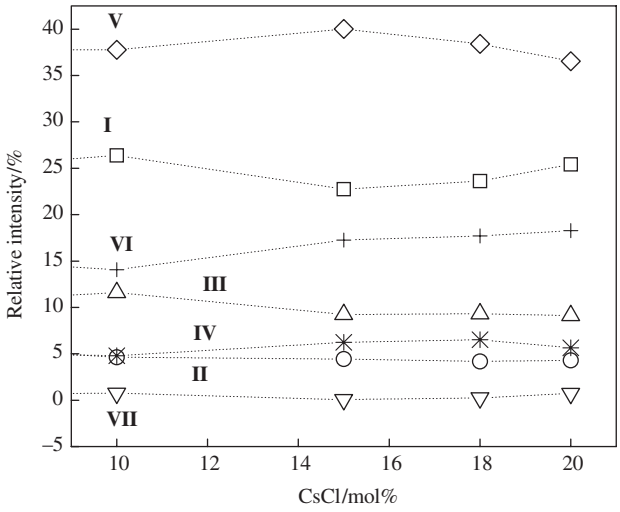

Fig. 9. Relative integrated intensity of each band (from I to VII) in the Raman spectra as a function of the CsCl content.

at 270 cm^{-1} (band IV—assigned to the bonding vibration of two edge-shared tetrahedra), a intense band at 324 cm^{-1} (band V—attributed to a stretching mode of the GaS_4 tetrahedron), a shoulder situated at 390 cm^{-1} (band VI—assigned to a stretching mode of edge-shared tetrahedra), and a weak band at 486 cm^{-1} (band VII—assigned to the vibrations of two GaS_4 tetrahedra connected by a common sulfur atom).

The Raman spectra are characteristic of glasses with low phonon frequencies, and there is no noticeable influence of the CsCl content on the Raman cutoff at 450 cm^{-1}.

IV. Discussion

Figure 1 shows that the glass density within statistical error does not change with the CsCl concentration. The linear refractive index, however, increases with the addition of CsCl, as shown in Fig. 6. This behavior is because of the presence in the glass network of Cs^+ ions, which have a higher polarizability than Na^+ ions. The refractive index values are much higher than the corresponding values for silica glass, which enhances the optical non-linearities as predicted by the Lines model.[8,9] For comparison, the refractive index of silica at 589.9 nm is 1.5, which is well below the values obtained for all samples at this wavelength. By using the Lines model, we have estimated high values for the optical non-linearity $\chi^{(3)}$ (Fig. 7), which could be a good indication of the suitability of the material to non-linear optical applications. Although this is only an estimate, the Lines model has already been successfully compared with experimental data.[19]

The thermograms of these glasses (Fig. 4) show that the thermal stability reaches a maximum at around 15 mol% of CsCl (the curve at this concentration was the smoothest). Figure 3 shows that the thermal expansion coefficient κ increases with the addition of CsCl for concentrations up to 18 mol%, which corresponds to the region of interest since, for higher concentrations, glass crystallization occurs. The increase in κ indicates that the bonds became weaker, i.e., the addition of CsCl produced Ga–Cl bonds that are weaker than the Ga–S bonds. It is known that weaker bonds increase the anharmonic contributions of the inter-ionic potentials to thermal expansion. This fact is corroborated by the absorption and by the T_g and T_d results. The blue shift of the Tauc curves (Fig. 5) with the increase of the Cl content is strong evidence that CsCl penetrates into the Ga–S glass structure. The Ga–S bonds are broken, increasing non-bridging S^- and producing Ga–Cl bonds. The Cl^- ions are more ionic than S^- ions and increase the Tauc gap of the glass. The increase of non-bridging S^- with increasing CsCl concentration is supported by the decrease of the T_g and T_d temperatures. The Cs^+ ions, similar to Na^+, locate around the non-bridging S^- to compensate charge. Extended X-ray absorption fine structure (EXAFS) and infrared measurements[20] have shown that there are no Cs^+ ions around Cl^- ions.

The overall shape of the Raman spectra does not show a significant change with the addition of CsCl. Each spectrum was then deconvoluted using seven Gaussian functions, considering the peak assignments reported above, and the relative integrated intensity of each band as a function of the CsCl content is plotted in Fig. 9. By performing this deconvolution, one can observe that the relative intensities of the bands do show changes with the CsCl content. Some bands present a maximum or a minimum at around 15 mol%. For example, the most intense band (band V—the stretching mode of the GaS_4 tetrahedron) presents a maximum at around 15 mol%. This behavior could be an indication that, for concentrations up to ~15 mol%, the Cl breaks up the GaS_4 tetrahedra forming terminal Cl while, for higher concentrations, the Cl enters the glass network forming Ga–Cl–Ga bonds, joining the tetrahedra.[20] To illustrate the

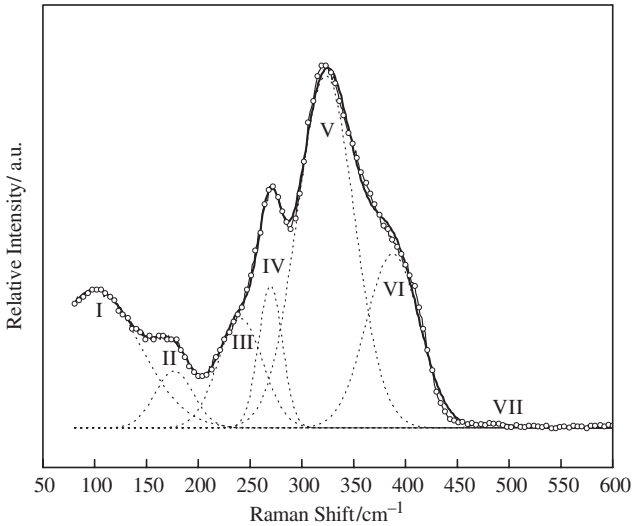

Fig. 10. Raman scattering spectrum of the 18 mol% CsCl sample (○). The dotted lines show the seven Gaussian functions resulting from spectrum deconvolution, and the solid line shows the fitting result.

Table IV. Fitting Results of η_o and E_a for Various Glasses

	High-temperature region		Low-temperature region	
Glass	η_o	E_a (kcal/mol)	η_o	E_a (kcal/mol)
Na_2–ZnO–TeO_2†	1.6×10^{-9}	33.6	1.4×10^{-21}	7.9
WO_3–TeO_2	1.6×10^{-11}	41.4	1.3×10^{-21}	1.9
Na_2O–SiO_2†	6.5×10^{-5}	31.8	6.2×10^{-8}	49
ZBLAN	4.4×10^{-12}	37.6	8.9×10^{-39}	103.6
Ga_2S_3–Na_2S–CsCl†	5.6×10^{-17}	90.0	1.2×10^{-20}	107.5

†Easy to draw optical fiber.

quality of the spectral deconvolution, Fig. 10 shows the Gaussian functions resulting from the deconvolution and the fitting result for the 18 mol% CsCl sample.

In the above discussion, we show that significant properties of the GNSC glass system, such as the thermal stability and the non-linear refractive index, increased with the addition of CsCl. In the following discussion another property, the activation energy for viscous flow, will be discussed.

As drawing of fiber is a process involving a dynamic deformation at high temperature, it is very important to know the behavior of the viscosity in the range of high and low temperatures.[21] From the Arrhenius plot of the viscosity (η_0), the activation energies (E_a) for viscous flow at both low and high temperatures are obtained. The difference between them indicates the differences in the glass deformation structure. The results are shown in Table IV. For comparison, this table includes the activation energy values for different glasses.

The results show that silicate glass presents the smallest (17.2 kcal/mol) difference between the activation energies at low and high temperatures, and the ZBLAN glass the largest (66 kcal/mol). The GNSC glass has a very small activation energy difference (17.5 kcal/mol), which is very close to the value for silicate glass. This is an important property of this glass system. The small activation energy difference is a favorable point in the direction of the fabrication of the optical fiber.

V. Conclusions

The GNSC glass system forms glasses with high homogeneity and stability. The refractive index and the thermal stability were found to increase with the addition of CsCl. The presence of CsCl in the glass system did not affect the Raman cutoff, characterizing a low-phonon energy glass. The system presents a small difference between the activation energy for viscous flow at low and at high temperatures, which is a desirable property for drawing optical fibers. Furthermore, the high estimated values for the third-order non-linear optical susceptibility at 1.5 and 1.3 μm suggest the potential use of these glasses in optoelectronic applications.

Acknowledgments

The authors are grateful to CNPq, FAPESP, and PRONEX for financial support, and to Prof. C.H. Collins (IQ-UNICAMP, Brazil) for the English revision of the paper. This is a contribution of the Millennium Institute for Complex Materials (PADCT/MCT).

References

[1]P. C. Becker, M. M. Broer, V. C. Lambrecht, A. J. Bruce, and C. Nykolak. "Pr^{3+}: La–Ga–S Glass: A Promising Material for 1.3 Micron Fiber Amplification"; p. 251–4 in *Teck Digest of Optical Society of America Proceedings*, Washington, DC, 1992

[2]B. Dussardier, D. W. Hewak, B. N. Sanson, H. J. Tate, J. Wang, and D. N. Payne, "Pr^{3+}-Doped Cs–Ga–S–Cl Glass for Efficient 1.3 μm Optical-Fiber Amplifier," *Electron. Lett.*, **31** [3] 206–8 (1995).

[3]R. Reisfeld and A. Bornstein, "Absorption and Emission-Spectra in Chalcogenide Glass of Composition $0.7Ga_2S_3$–$0.27La_2S_3$–$0.03Nd_2S_3$," *Chem. Phys. Lett.*, **47** [1] 194–6 (1977).

[4]D. W. Hewak, R. S. Deol, J. Wang, G. Wylangowski, J. A. Medeiros Neto, B. N. Samson, R. I. Laming, W. S. Broklesby, and D. N. Payne, "Low Phonon-Energy Glasses for Efficient 1.3 μm Optical-Fiber Amplifiers," *Electron. Lett.*, **29** [2] 237–9 (1993).

[5]J. Wang, H. R. Hector, D. Brady, D. Hewak, B. Brocklesby, M. Kluth, R. Moore, and D. N. Payne, "Halide-Modified Ga–La Sulfide Glasses with Improved Fiber-Drawing and Optical Properties for Pr^{3+}-Doped Fiber Amplifiers at 1.3 μm," *Appl. Phys. Lett.*, **71** [13] 1753–5 (1997).

[6]M. Palazzi, "Study of the System Ga_2S_3–Na_2S-Existence a Glass-Former Regions," *C. R. Acad. Sci.*, **299** [9] 529–32 (1984).

[7]K. Itoh, H. Yanagita, H. Tawarayama, K. Yamanaka, E. Ishikawa, K. Okada, H. Aoki, Y. Matsumoto, A. Shirakawa, Y. Matsuoka, and H. Toratani, "Pr^{3+} Doped InF_3/GaF_3 Based Fluoride Glass Fibers and Ga–Na–S Glass Fibers for Light Amplification Around 1.3 μm," *J. Non-Cryst. Solids*, **256–257**, 1–5 (1999).

[8]M. E. Lines, "Influence of d-Orbitals on the Nonlinear Optical-Response of Transparent Transition-Metal Oxides," *Phys. Rev. B*, **43** [14] 11978–90 (1991).

[9]M. E. Lines, "Bond-Orbital Theory of Linear and Nonlinear Electronic Response in Ionic-Crystals. 2. Nonlinear Response," *Phys. Rev. B*, **41** [6] 3383–90 (1990).

[10]E. M. Marmolejo, E. Granado, O. L. Alves, C. L. Cesar, and L. C. Barbosa. "Fabrication of Ga_2S_3 Based Glasses in Sulphur Flowing Atmosphere"; pp. 34–38 in XVIII *International Congress on Glass Proceedings*, San Francisco, CA, 1998.

[11]S. J. Wilson and D. Poole, "Glass Viscosity Measurement by Parallel Plate Rheometry," *Mater. Res. Bull.*, **25** [1] 113–8 (1990).

[12]A. Y. Ramos, O. L. Alves, C. L. Cesar, and L. C. Barbosa, "Structural Characterisation of CsCl Incorporation in Ga_2S_3–La_2S_3 Glasses," *J. Non-Cryst. Solid*, **304** [1–3] 182–7 (2002).

[13]S. K. J. Alani, C. A. Hogarth, and R. A. El Malawany, "A Study of Optical-Absorption in Tellurite and Tungsten Tellurite Glasses," *J. Mater. Sci.*, **20** [2] 661–7 (1983).

[14]J. Tauc, R. Grigorovici, and A. Vancu, "Optical Properties and Electronic Structure of Amorphous Germanium," *Phys. Status Solidi*, **15** [2] 627 (1966).

[15]S. H. Wemple and M. DiDomenico Jr., "Behavior of Electronic Dielectric Constant in Covalent and Ionic Materials," *Phys. Rev. B*, **3** [4] 1338 (1971).

[16]K. Nassau, "Materials Dispersion Zero in Glass Mixtures," *Electron. Lett.*, **17** [20] 768–9 (1981).

[17]K. Nassau, "The Material Dispersion Zero in Infrared Optical-Waveguide Materials," *Bell. Syst. Tech. J.*, **60** [3] 327–37 (1981).

[18]S. Barnier, M. Palazzi, M. Massot, and C. Julien, "Vibrational-Spectra of the Vitreous Ga_2S_3–Na_2S System," *Solid State Ionics*, **44** [1–2] 81–6 (1990).

[19]L. Canioni, L. Sarger, P. Segonds, A. Ducasse, C. Duchesme, E. Fargin, R. Olazeuaga, and G. Le Flem, "Experimental and Theoretical Investigation of Highly Nonlinear Optical-Glasses," *Solid. State. Comm.*, **84** [11] 1065–7 (1992).

[20]J. R. Hector, J. Wang, D. Brady, M. Kluth, D. W. Hewak, W. S. Brocklesby, and D. N. Payne, "Spectroscopy and Quantum Efficiency of Halide-Modified Gallium–Lanthanum Sulfide Glasses Doped with Praseodymium," *J. Non-Cryst. Solid*, **239** [1–3] 176–80 (1998).

[21]J. S. Wang, E. M. Vogel, and E. Snitzer, "Tellurite Glass: A New Candidate for Fiber Devices," *Opt. Mater.*, **3** [3] 187–203 (1994). □